Intermolecular Hydrogen Bonding and Vibrational Analysis of *N,N*-Dimethylformamide Hexamer Cluster

Sun-Kyung Park, Kyung-Chul Min, Choongkeun Lee, Soon Kang Hong,† Yunsoo Kim,‡ and Nam-Soo Lee*

Department of Chemistry, Chungbuk National University, Cheongju, Chungbuk 361-763, Korea
**E-mail: nslee@chungbuk.ac.kr*
†Department of Fire Service Administration, Chodang University, Chonnam 534-701, Korea
‡Department of Advanced Materials Chemistry, Korea University, Jochiwon 339-700, Korea
Received July 16, 2009, Accepted September 10, 2009

Hexamer cluster of *N,N*-dimethylformamide(DMF) based on the crystal structure was investigated for the equilibrium structure, the stabilization energies, and the vibrational properties in the density functional force field. The geometry (point group C_i) of fully optimized hexamer clustered DMF shows quite close similarity to the crystal structure weakly intermolecular hydrogen bonded each other. Stretching force constants for intermolecular hydrogen bonded methyl and formyl hydrogen atoms with nearby oxygen atom, methyl C–H···O and formyl C–H···O, were obtained in 0.055 ~ 0.11 and ~ 0.081 mdyn/Å, respectively. In-plane bending force constants for hydrogen bonded methyl hydrogen atoms were in 0.25 ~ 0.33, and for formyl hydrogen ~ 0.55 mdynÅ. Torsion force constants through hydrogen bonding for methyl hydrogen atoms were in 0.038 ~ 0.089, and for formyl hydrogen atom ~ 0.095 mdynÅ. Calculated Raman and infrared spectral features of single and hexamer cluster represent well the experimental spectra of DMF obtained in the liquid state. Noncoincidence between IR and Raman frequency positions of stretching C=O, formyl C–H and other several modes was interpreted in terms of the intermolecular vibrational coupling in the condensed phase.

Key Words: *N,N*-dimethylformamide, Hexamer cluster, Vibrational analysis, Intermolecular hydrogen bonding, Intermolecular vibrational coupling

Introduction

DMF (*N,N*-dimethylformamide, $(CH_3)_2NCHO$) is a hydrophilic aprotic solvent with a high boiling point and very polar with a large dipole moment 3.82 D. DMF molecule has a planar skeletal geometry which has been a subject of theoretical, computational and experimental investigations over the years.[1~8] A slight non-planarity in the gas phase was reported by gas phase electron diffraction method,[5] which indicated some attractive intramolecular interaction between oxygen atom and methyl hydrogen atom syn to carbonyl group where the distance is quite near, only 2.4 Å. However, in the liquid or solid state, it was investigated to be planar in the skeletal geometry. In addition, it has some interesting structural characters, i.e., a simplicity in the chemical structure, a low molecular symmetry (point group C*s* if assuming planar), and an intermolecular interaction capability to its neighbors in the condensed phase considering its physical properties. Geometric configuration of DMF could be qualitatively viewed by considering following resonance forms to explain its distinctive structural feature, a skeletal planarity.

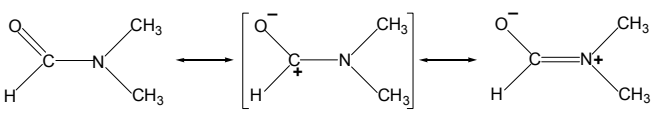

In the liquid state, it is generally considered fully disordered, but a partially ordered structure was suggested to form a cluster, possibly a dimer.[8] The bond length of C=O bond 1.24 Å in the liquid[4] state obtained through X-ray diffraction study[1] is slightly, about 0.02 Å, longer than in the gas state,[5] while the bond length of formyl C–N bond 1.35 Å in liquid is a bit, about 0.01 Å, longer than in crystal, but 0.04 Å shorter than in the gas state. Others, two methyl C–N bonds, 1.45 Å, are similar to those in the gas and crystal state. In the crystal structure, the cluster of DMF was formed and connected by weak C–H···O hydrogen bonds, all of which with oxygen atoms as hydrogen bond acceptor. In the crystal structure at 90 K, the mean distance of C=O bond was 1.23 Å, formyl C–N bond 1.34 Å, and methyl C–N bonds 1.453 Å. The variance of the bond lengths in different states indicates that a strong intermolecular interaction exercises cooperatively between neighboring molecules in the condensed phases. The structural study[1] of DMF crystal and liquid phases showed that the less positively charged formyl proton of DMF in the hexamer cluster allows formation of weak hydrogen bonds in the solid state, which are comparable in strength with interactions between the methyl protons and oxygen atoms.

The intermolecular nonbonding interaction in the condensed phase could be understood to be electrostatic and/or dipole-dipole interaction due to its high dipole moment, and other types of weak interactions such as dispersive forces. Among weak interactions, the intermolecular hydrogen bonding interaction of C–H···O is known to be very weak, but its existence of this kind of nonbonding[8~10] was provided specifically in some organic crystal structures. The hydrogen bond distances observed frequently less than 2.4 Å in some crystal structures. Because the van der Waals distance of this bond is near 2.6 Å, it could be regarded as a certain amount of hydrogen bonding interaction. Under some circumstances, C–H could be a donor

to form a soft hydrogen bond. It has been focused because this weak nonbonding interaction could be potential in the fields of the supramolecular chemistry and the structural biology of biological macromolecules.

The normal mode analysis is a method based on the analytic dynamics of a chemical system whose potential energy is expressed as a quadratic function, i.e., harmonic potential approximation, of atomic displacement from its equilibrium geometry. A normal mode comes from a concerted motion of interconnected atoms. The normal mode analysis of a cluster system can provide direct information of weak nonbonding by way of generating force constants of concerned. This type of low energy interaction has been proven valuable in modeling slow conformational dynamics of biological molecular structures because the force constants of low energy nonbonding interactions should be incorporated for the study of molecular dynamics simulation using empirical force fields at the atomic level.

In the present study, the vibrational analysis of hexamer cluster of six DMF molecules based on the crystal structure[1] was investigated by the normal mode analysis of Wilson's *GF* matrix formulation[11,12] using local symmetry coordinates. We employed the method of density functional BP86 approximation which has been successfully applied for the vibrational prediction of many nitrogen compounds because it is more accurate for the vibrational frequency calculations than any other density functional formalism. The polarization and diffuse functions were adapted to consider the significant charge separation in DMF molecules. The calculation results were compared to the experimental spectroscopic Raman or infrared data. The hydrogen bonding effects between neighboring molecules in the hexamer cluster were studied by obtaining the force constants of stretching, bending, and torsion modes as well in energetic and structural points of view.

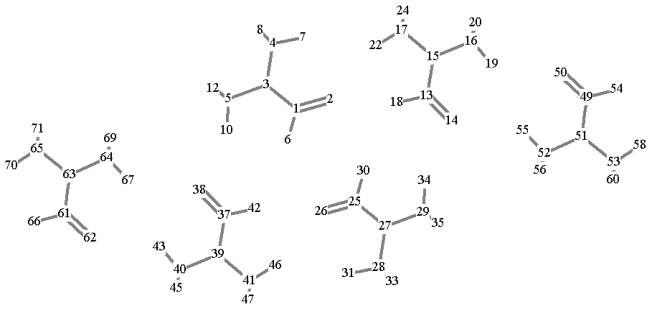

Figure 1. Hexamer cluster of DMF with index numbers and hydrogen bonds between DMF molecules (Dashed lines represent weak hydrogen bonds.) Cluster was classified into three groups. Group A: index number 1~12 and 25~36, Group B: index number 13~24 and 37~48, Group C: index number 49~60 and 61~72.

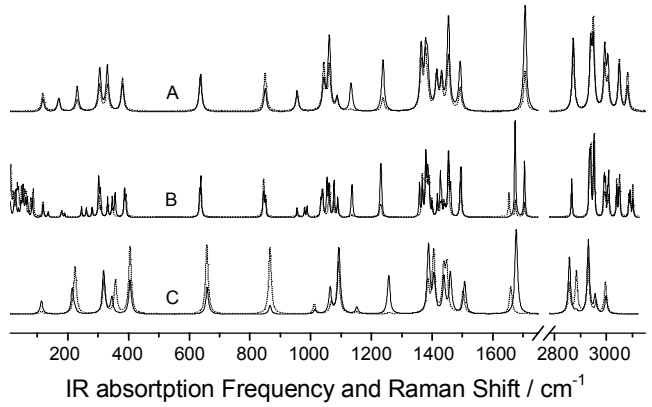

Figure 2. Raman(dot line) and IR(straight line) spectra of DMF. (A: calculated spectra of single DMF, B: calculated spectra of DMF hexamer cluster, C: experimentally observed spectra of liquid state DMF constructed from data presented in *ref. 2*(*a*).

Computational Details

Cluster model. Initial structure of cluster was generated using CS CHEM3D PRO (CambridgeSoft Cooperation) according to the crystal structure reported previously, and then transferred to the Gaussian03 program package for the optimization and the frequency calculation. Fully optimized structure displayed in Figure 1 was obtained without any structural constraints at various levels of theory, and then employed for the calculation of Cartesian force constants and the intensities of Raman and infrared normal modes. The hexamer cluster was not positioned perfectly planar, but slightly tilted holding C_i symmetry as shown in the crystal structure.

Single molecule and hexamer cluster of DMF were calculated at the theory level of B3LYP and BP86 using the 6-31+G** basis sets with the Gaussian03 program package (Gaussian, Inc.). The isotope atomic masses adapted for calculations were 12.01115 for carbon, 14.00307 for nitrogen, 15.9994 for oxygen, and 1.007825 for hydrogen, respectively. The temperature was set to 298.15 K and the pressure to 1.0 atm. The infrared and Raman spectra calculated for single and hexamer cluster are shown in Figure 2 along with experimental spectra constructed data taken from ref. 2(a). Because the hexamer cluster possesses its point group C_i symmetry, the cluster was classified into three groups for the convenience. The group A is of atom index number 1 ~ 12 and 25 ~ 36; the group B of atom index number 13 ~ 24 and 37 ~ 48; the group C of atom index number 49 ~ 60 and 61 ~ 72.

Normal mode analysis. The local symmetry coordinates of single DMF molecule (C_s point group) was composed of 11 stretching, 14 in-plane bending, 2 out-of-plane deformation, and 3 torsion vibrations. These were the same as reported previously. The fundamental vibrational modes are split into 19 A' and 11 A" symmetry species. To obtain vibrational properties of hydrogen bonds in the hexamer cluster (C_i point group), each single molecule was configured to be connected each other through hydrogen bonds displayed in Figure 1. The local symmetry coordinates were composed of 70 stretching, 92 in-plane bending, 12 out-of-plane deformation, and 30 torsion vibrations. Single DMF molecule and hexamer cluster have 12 and 72 atoms in total, respectively. The force constants matrix in the Cartesian coordinate generated through density functional calculation has 666 and 23436 elements for single molecule and hexamer cluster overall which are composed of all the diagonal and half the off-diagonal elements. Using these elements, the force constants in the local symmetry coordinates, the frequencies, and potential energy distributions were obtained using

Table 1. Structural bond lengths in gas, liquid and crystal, and Optimized molecular parameters of DMF single and hexamer cluster at B3LYP and BP86 level of theory.

Bond Length/Å	Experimental			B3LYP/6-31+G**			BP86/6-31+G**		
	Gas[a]	Liquid[b]	Crystal[c]	single	hexamer[d]		single	hexamer[d]	
					Group A, B	Group C		Group A, B	Group C
C=O	1.224	1.24	1.231	1.225	1.236	1.226	1.235	1.246	1.236
C-N	1.391	1.35	1.340	1.364	1.356	1.360	1.374	1.366	1.370
N-CH_3 syn to O	1.453	1.45	1.452	1.455	1.455	1.458	1.459	1.460	1.462
N-CH_3 syn to H	1.453	1.45	1.453	1.452	1.456	1.452	1.456	1.461	1.457
C-H formyl	1.112 mean	1.09	0.980	1.106	1.101	1.106	1.117	1.112	1.117
C-H_3 syn to O			0.950	1.090	1.089	1.089	1.100	1.099	1.099
C-H_3 syn to H			0.972	1.093	1.092	1.093	1.102	1.103	1.117

[a]Experimental data from *ref.5*. (unit: Å). [b]Experimental data from *ref.4*. (unit: Å). [c]Experimental data from *ref.1*. (unit: Å). [d]group A, B and C classification as shown in Figure 1.

Table 2. Stabilization Energy (kJ/mol) per a DMF molecule at 298 K and 1 atm of Hexamer cluster at B3LYP and BP86 level of theory.

	Energy[a]	Single/hartree	Hexamer/hartree	Stabilization[c] /kJ/mol
B3LYP/6-31+G**	E_o	–248.431	–1490.612	–10.80 (-8.90)
	E_T	–248.425	–1490.565	–6.42 (-5.62)
	ΔG^b	–248.431	–1490.678	–40.88 (-36.65)
BP86/6-31+G**	E_o	–248.431	–1490.603	–7.58 (-6.46)
	E_T	–248.425	–1490.555	–3.18 (-2.82)
	ΔG^b	–248.431	–1490.670	–38.11 (-33.45)

[a]E_o (electronic + zero point energy) and E_T (electronic + thermal energy) $\cong \Delta H$. [b]Vibrational entropy was only counted, so the rotational and translational entropy were ignored for the Gibbs free energy calculation. [c]The stabilization energies $\Delta(E_o)$, $\Delta(E_T)$ and $\Delta(\Delta G)$ are in kJ/mol unit, and defined as [Δ(hexamer)-6Δ(single)]/6. The values in parenthesis are the stabilization energies obtained from the counterpoise corrected calculation for the superposition errors in the basis set (BSSE).

Wilson's *GF* matrix method. In this study, we did not apply any scaling factor, e.g., 0.96, *etc.*, for the frequency calculations partly because the intermolecular interaction and dipolar coupling in the hexamer cluster adjust and/or affect the whole structural parameters of molecules. Others were the same as previously reported.[12]

Results and Discussion

Optimized structure of DMF hexamer cluster. Mean bond distances of fully optimized geometry of DMF hexamer cluster at the level of B3LYP and BP86 theory using 6-31+ G** basis set have been presented in Table 1 with those of fully optimized DMF single. Gas, liquid and X-ray crystallographic data of crystal state were included. Every DMF single molecule in the cluster was planar in the optimized geometry, as well as in the single molecule. The skeletal inter-planar angle for hexamer was obtained to have 178.1° at B3LYP level, and 178.7° at BP86 level. This angle is similar to the crystal geometry, where the angle of 170.9° was observed.[1]

The carbonyl bond length varies upon the physical state of DMF as much 0.01 Å, i.e., 1.22 Å (gas), 1.24 Å (liquid) and 1.23 Å (crystal). Further, the bond length of C–N connected next to carbonyl group decrease upon the states, 1.39 Å (gas), 1.35 Å (liquid) and 1.34 Å (crystal). The bond lengths C–H of formyl and methyl groups also decrease on the states, 1.112 Å (gas), 1.09 Å (liquid) and ~0.98 Å (crystal). The lengthening of C=O, shortening of both C–N and C–H bond distances in the condensed phase indicate the strong intermolecular interaction. In the calculated geometry, the same features were observed, but not as much as the experimentally observed structural. However, the four-membered centro-symmetric ring entity (group A and B in Table 1 and Figure 1) inside the hexamer cluster shows above experimental measures clearly. The bond lengths of C–H in crystal are noticeably shorter than liquid or gas partly because the distance of hydrogen atom inherently comes shorter through the crystal packing.

Energetics of DMF hexamer cluster. Intermolecular interactions would generate significant stabilization energies to form the cluster. Table 2 shows these results at two levels of theory, B3LYP and BP86 using 6-31+G** basis set under 1.0 atm and 298 K. Because clustering could generate a lot of low frequencies from concerted vibrational motions in the cluster, the vibrational contribution become larger upon more clustering. These low vibrational frequencies generated due to clustering shows two different effects, i.e., moderate stabilization in enthalpy (or internal energy) and large stabilization in free energy. The thermal correction of vibrational component to the internal energy, $\Delta U_{vib}(T)$, would be quite large for clustering due to considerable contribution of low frequencies. It would

Table 3. Calculated Frequencies of DMF single and hexamer at BP86 level, and experimental Raman and infrared frequencies of liquid DMF with Assignments.

	Experimental		DMF single	DMF hexamer		Assignments[d]
	Raman[b]	IR[b]		Raman[c]	IR[c]	
ν1	2996	2998	3081	3086(A), 3092(C), 3101(B)	3086(A), 3092(C), 3101(B)	$\nu_{as}(CH_3)^O$
ν2	2960	2956	3050	3039(A), 3047(C), 3051(B)	3039(A), 3047(C), 3051(B)	$\nu_{as}(CH_3)^H$
ν3	2929	2930	2950	2951(A), 2952(C), 2954(B)	2951(A), 2952(C), 2954(B)	$\nu_{s}(CH_3)^O$
ν4	2884	2884	2940	2935(A), 2937(B), 2940(C)	2934(A), 2937(B), 2940(C)	$\nu_{s}(CH_3)^H$
ν5	2856	2857	2872	2867(C), 2933(B), **2941(A)**	2867(C), 2933(B), **2938(A)**	ν(C1-H)
ν6	1659	1677	1707	**1654(A)**, 1674(B), 1705(C)	**1673(A)**, 1674(B), 1705(C)	ν(C=O) + ν(C1-N)
ν7	1502	1507	1493	1492(A), 1494(C), 1496(B)	1493(C), 1494(A), 1496(B)	$\delta_{as}(CH_3)^H + \delta_{as}(CH_3)^O$
ν8	1448	1460	1455	1453(A), 1454(B), 1455(C)	1453(A), 1454(B), 1455(C)	$\delta_{as}(CH_3)^O + \delta_{as}(CH_3)^H$
ν9	1438	1440	1416	1417(C), 1427(B), 1428(A)	1417(C), 1427(B), 1428(A)	$\delta_{s}(CH_3)^H$
ν10	1405	1406	1386	1379(B), 1380(A), 1391(C)	1379(B), 1380(A), 1391(C)	$\delta_{s}(CH_3)^O$ + δ(C-H)
ν11	1386	1388	1378	1381(C), 1385(B), 1389(A)	1381(C), 1385(B), 1389(A)	ν(C1-N) + $\delta_{s}(CH_3)^H$
ν12	1386	1388	1364	**1367(A)**, 1368(C), 1400(B)	**1358(A)**, 1368(C), 1400(B)	δ(C-H) + ν(N-C4)
ν13		1257	1239	1229(B), 1232(C), 1233(A)	1229(B), 1232(C), 1233(A)	ν(N-C5) + ν(N-C4)
ν14	1091	1093	1062	1040(A), 1060(C), 1076(B)	1040(A), 1060(C), 1077(B)	$\rho(CH_3)^H + \rho(CH_3)^O$
ν15	1068	1064	1043	1034(B), 1038(C), **1054(A)**	1034(B), 1038(C), **1063(A)**	$\rho(CH_3)^O + \rho(CH_3)^H$
ν16	866	866	851	845(C), 847(B), 852(A)	845(C), 847(B), 852(A)	ν(N-C4) + ν(N-C5)
ν17	658	659	638	**636(A)**, 638(C), 639(B)	**634(A)**, 638(C), 640(B)	δ(OCN) + ν(N-C5)
ν18	405	405	380	387(A), 388(C), 392(B)	387(A), 388(C), 392(B)	δ(C4NC5)
ν19	319	318	305	302(C), 304(B), **310(A)**	302(C), 303(B), **307(A)**	δ(C1NC5) + δ(OCN)
ν20	2996	2998	3005	3005(A), 3009(B), 3009(C)	3005(A), 3009(B), 3009(C)	$\nu_{as}(CH_3)op^O$
ν21	2960	2956	2993	2951(A), 2952(C), 2954(B)	2951(A), 2952(C), 2954(B)	$\nu_{as}(CH_3)op^H$
ν22	1448	1460	1454	1453(B), 1457(A), 1461(C)	1454(B), 1457(A), 1462(C)	$\delta_{as}(CH_3)op^O$
ν23	1438	1439	1431	1432(C), 1439(B), 1444(A)	1432(C), 1439(B), 1444(A)	$\delta_{as}(CH_3)op^H$
ν24		1152	1133	1135(C), 1137(B), 1138(A)	1135(C), 1137(B), 1138(A)	$\rho(CH_3)op^O + \rho(CH_3)op^H$
ν25	1091	1093	1087	1089(C), 1090(A), 1090(B)	1089(C), 1090(A), 1090(B)	$\rho(CH_3)op^H + \rho(CH_3)op^O$
ν26	1012	1014	956	955(C), 980(A), 989(B)	955(C), 980(A), 989(B)	δ(C-H)op
ν27	357	345	330	332(C), 346(B), **350(A)**	332(C), 346(B), **356(A)**	τ(C1-N3)
ν28	224		232	246(C), 261(B), 281(A)	246(C), 261(B), 281(A)	τ(N3-C5) + δ(CNC)op
ν29		215	171	179(A), 182(C), 190(B)	180(A), 182(C), 190(B)	τ(N3-C5) + δ(N3-C4)
ν30		113	118	118(A), 120(C), 136(B)	118(A), 120(C), 136(B)	δ(CNC)op + τ(N3-C4)

[a]Vibrations ν1 ~ ν19; A' symmetry, vibrations ν22 ~ ν30; A" symmetry in DMF single. [b]Experimental data taken from *ref.* 2(a). [c]The band pairs in which the vibrational coupling occurs noticeably are typed in the **bold** face. [d]symbol ν: stretching, δ: deformation, ρ: rocking, τ: torsion, op: out-of-skeletal plane, subscript s: symmetric, subscript as: anti-symmetric, superscript O: syn to oxygen atom, superscript H: syn to formyl H atom.

increase the total internal energy of the cluster, consequently the total enthalpy, which results in moderate stabilization in enthalpy. However, these low frequencies increase also the total entropy a great deal to derive the free energy considerably low. Considering the stabilization in a condensed phase, the contributions of rotational and translational entropy to total entropy were ignored for the total free energy. Therefore the vibrational entropy was only counted to obtain the Gibbs free energy as following formulas.

$$\Delta H = \Delta U + \Delta(PV) = E_o + \Delta U(T) + \Delta(PV) \cong E_o + \Delta U(T) = E_T$$

E_o = electronic + zero point energy

E_T = electronic + thermal energy

$$\Delta U(T) = \Delta U_{trans}(T) + \Delta U_{rot}(T) + \Delta U_{vib}(T)$$

$$\Delta G = \Delta H - T\Delta S_{tot}$$
$$= \Delta H - T\Delta(S_{trans} + S_{rot} + S_{vib} + \ldots) \cong \Delta H - T\Delta(S_{vib} + \ldots)$$

Stabilization energies in ΔH ($\cong E_T$ in a condensed phase) per a single DMF molecule was, as expected, calculated in the range of about –5 kJ/mol for hexamer. However, the stabilization free energy ΔG was obtained to be about – 40 kJ/mol as shown in Table 2. If we consider the lager cluster, the stabilization free energies would be greater even.

Vibrational analysis of DMF hexamer cluster: Calculated infrared and Raman spectra of DMF single and hexamer cluster at BP86/6-31+G** level with experimental frequencies of liquid DMF in Figure 2 and Table 3. The band pairs in which the intermolecular vibrational coupling occurs noticeably are

typed in the bold face. The frequency results of B3LYP functional were not good enough for the analysis, so those of BP86 functional were analyzed. Normal mode analysis of single DMF molecule had been extensively studied previously by several groups, and every mode of its 30 normal modes had been well defined. Our results for single DMF were the same as previous studies.[2,3]

Vibrations of C=O stretching region: The characteristic feature of an amide species is the amide I band, which is mainly attributed to C=O stretching and associated with C–N stretching and weakly with C–H in-plane bending. Stretching frequencies (ν6) of C=O were calculated at 1654 cm^{-1} in Raman and at 1673 cm^{-1} in IR for group A of the hexamer cluster. For group B and C, they show at 1674 and 1705 cm^{-1}, respectively. They are all well below down-shifted compared to amide I band of isolated DMF. Amide I band of isolated DMF in the liquid phase[13] was measured at 1724 cm^{-1} by diluting DMF in CCl_4 solution. In addition, considering they are spread in three parts, these three groups show different extent of perturbation for their potential curves induced from their own intermolecular interactions.

For group A, two carbonyl bonds couples strongly because they are near each other oppositely facing in parallel and very polar. As a consequence, the in-phase (Raman active) and out-of-phase stretching (IR active) mode shows positive noncoincidence effect (NCE),[14~18] in this case $\Delta\omega = 19$ cm^{-1}. This effect is known to be as $\Delta\omega = \omega_{aniso} - \omega_{iso} \cong \omega_{ir} - \omega_{iso}$ because the IR peak frequencies are approximately coincident with the anisotropic Raman lines.[14] The intensity of isotropic Raman line is much higher than anisotropic for the polarized Raman lines. This value is quite comparable to 17 cm^{-1} calculated with a time-domain computation method.[18] Delocalization of vibrational energy or splitting of a degenerated vibrational level for a certain mode by means of vibrational coupling[19~21] are often considered by two kinds of mechanism, *i.e.*, couplings through bond and through space. This NCE observed in group A is almost completely through the space coupling due to intermolecular coupling of dipolar bonds. The effect through bond is weak compared to through space as can be seen in following table which is from BP86/6-31+G** calculation of hexamer cluster.

C=O stretching force constant (unit: mdyn/Å)	Group A in-phase	Group B in-phase	Group C in-phase	Group A out-of-phase	Group B out-of-phase	group C out-of-phase
group A in-phase	10.7946					
group B in-phase	–0.1105	10.8393				
group C in-phase	0.0130	–0.0284	11.4331			
group A out-of-phase				10.9222		
group B out-of-phase				0.0120	10.8715	
group C out-of-phase				0.0039	–0.0346	11.4345

The in-phase and out-of-phase C=O stretching vibrations of group A, B and C in the diagonal elements show very large values of force constants, near in the range of 10 ~ 11 mdyn/Å as shown in table above. In contrast, the interaction force constants in the off-diagonal elements are relatively small, about 0.1 or less. For group C, the diagonal force constants of in-phase and out-of-phase mode are not much different, indicating the coupling is very weak. The mixing between group A and C would be very weak partly because of their positional effect, nearly anti-parallel and far apart. Between group B and C, they couple in moderate way because they are in parallel, still very small due to orientation angle dependence of two dipolar interactions in parallel, $(1 - 3\cos^2\theta$, angle $\theta = 52.8$ degree between two parallel carbonyl groups of group B and C). Between group A and B, small extent of mixing occurs in the in-phase stretching vibrations, but weak enough in the out-of-phase stretching vibrations. The diagonal force constants of group A, in-phase (10.7946 mdyn/Å) and out-of-phase (10.9222 mdyn/Å) of C=O stretching vibrations show considerable difference for the most part responsible for positive high NCE.

Vibrations of formyl C-H stretching and deformation region: Stretching frequencies (ν5) of formyl C–H show a splitting at 2941 cm^{-1} in Raman in-phase mode and at 2938 cm^{-1} in IR out-of-phase for group A, whereas no splitting both for group B at 2933 cm^{-1} and for group C at 2867 cm^{-1}. In this case, the NCE value $\Delta\omega$ is small and negative value, –3 cm^{-1}. Because C–H bond is weakly dipolar, the extent of intermolecular coupling is expected to be very small. It was proposed that when liquid structures are dominated by non-polar forces as those present in H-bonded liquids (as C–O stretching mode[17] of methanol) the IR active modes may give rise to negative NCE. The delocalization of vibrational energy in the repulsive potential region caused by steric repulsive interactions (such as ring breathing mode of benzene) results in the negative non-coincidences. On the other hand, the resonance energy transfer arising due to the transition dipole-dipole (and induced dipole-induced dipole) interactions causes mainly positive noncoincidence (as O–H stretching mode of methanol,[17] carbonyl of acetone[15] or amide I of peptide,[20] *etc*). This small and negative value, –3 cm^{-1} observed in the formyl C–H stretching of group A seems to be caused by steric repulsive interactions because this stretching is mixed weakly in the intramolecular manner with $C–H_3$ stretching syn to formyl hydrogen atoms and in the intermolecular manner with formyl hydrogen atoms of group B.

The blue-shift of stretching frequency of X–H caused by intra/intermolecular interactions as X–H···Y types has been well studied and reported as the improper blue-shifting hydrogen bond.[22~24] The structural change of DMF induced by the water hydrogen bonded on the carbonyl group has been exclusively studied responsible for the methyl C–H blue-shift.[25~28] Taking a look at only calculated results for single and hexamer,

Table 4. Optimized structural parameters and Calculated force constants in the local symmetry coordinates (mdyn/Å for stretching, and mdynÅ for bending or torsion) of intermolecular hydrogen bonding in DMF hexamer cluster at B3LYP and BP86 level.

	Atoms[a]	Experimental	B3LYP/6-31+G**		BP86/6-31+G**	
		Crystal[b]	Structure[c]	Force Constant	Structure[c]	Force Constant
Stretching	r(H18···O2)	2.418 Å	2.380	0.0906	2.399	0.0810
	r(O14···H55)	2.647 Å	2.520	0.0759	2.573	0.0550
	r(H43···O62)		2.480	0.0919	2.503	0.0693
	r(O38···H10)	2.446 Å	2.322	0.1113	2.305	0.1084
Bending	θ(2,18,13)	149.3°	167.21	0.5267	164.56	0.5514
	θ(14,55,52)	144.7°	142.09	0.3264	141.05	0.2886
	θ(62,43,40)		140.84	0.4035	138.77	0.3300
	θ(38,10,5)	167.3°	158.29	0.2764	157.39	0.2553
Torsion	τ(1,2,18,13)	170.9°	178.05	0.0723	178.69	0.0957
	τ(13,14,55,52)		-178.02	0.0384	176.32	0.0403
	τ(61,62,43,40)		178.78	0.0440	-176.47	0.0381
	τ(5,10, 38,37)		179.29	0.0888	-179.11	0.0890

[a]The numbers are atomic index numbers shown in Figure 1. [b]Taken from *ref. 1.* [c]Hydrogen bond lengths (r) are in Å unit, and bond angles (θ) and torsion angles (τ) in degree unit.

the C–H frequencies of Group A and B show anomalous blue-shifts of about 68 and 61 cm^{-1} compared to DMF single, respectively. In contrast, it gives 5 cm^{-1} of red- shift in group C. The formyl hydrogen atoms at groups A and B are in the environments of close contact with others while that of group C is free from direct contact with other atoms. The subtle interplay between electrostatic attraction and steric repulsion was suggested to be responsible for blue shift effects in C–H···Y interactions. This mechanism of the blue shift of the C–H stretching frequency suggests that the effect could be enhanced by sterically induced compression of the C–H···Y bridging which may arise in the case of intramolecular contacts.

While the out-of-plane deformation (ν26) does not show any noticeable splitting, the in-plane bending (ν11) shows a negative splitting of −9 cm^{-1} for group A. During the in-plane bending of C–H bond in group A, two hydrogen atoms move each other head-on in the in-phase mode (Raman active), whereas the two lean to one side in the out-of-phase mode (IR active). This also could be interpreted as the repulsive potential effect caused by steric repulsive interactions.

Vibrations of C–N stretching region: Stretching frequencies (ν13, ν16) of C–N bonds are fairly localized except the C1–N stretching. The stretching frequencies (ν11) of C1–N bonds among three groups are up-shifted compared to the DMF single, indicating that intermolecular interaction makes it shorter and stronger particularly for group A and B. This bond are strongly coupled to the C=O bond to form amide I band, so this mode is dispersed in several bands. Two modes ν13 and are contributed mainly to anti-symmetric and symmetric stretching of N–C bonds, respectively. Both are down-shifted compared to the DMF single. These stretching frequencies did not show any significant NCE.

Vibrations of methyl C–H_3 stretching and deformation region: Stretching frequencies (ν1, ν2, ν3, ν4, ν20, ν21) of C-H_3 bonds are localized. Anti-symmetric stretching (ν1) of C-H_3 bonds syn to oxygen atom holding A' symmetry is spread out widely in the range of 15 cm^{-1} due to the steric interaction, but others not. Bending (ν7, ν8, ν9, ν10, ν22, ν23) and rocking (ν 14, ν15, ν24, ν25) of the C–H_3 bonds are also fairly localized except ν7 and ν15. The anti-symmetric bending (ν7) and in-skeletal plane rocking (ν15) deformations show moderate positive Δω values of 2 cm^{-1} and 9 cm^{-1} for group A only, respectively. This mode is combined in minor extent with skeletal stretching of delocalized C_2–N–C=O entity of group A.

Vibrations of skeletal in-plane bending region: Bending frequencies (ν17, ν18, ν19) of frame entity C_2–N–C=O are slightly delocalized in the negative way. When the skeletal frame of N–C=O in group A is doing a bending motion, in the cases of ν17 and ν19, the orientation angle of two C=O bonds changes continuously in-phase. It could be understood that it perturbs the intermolecular interaction to show moderate negative splitting in the skeletal in-plane bending of group A.

Vibrations of skeletal out-of-plane deformation and torsion region: The torsion and skeletal out-of-plane deformation modes (ν27, ν28, ν29, ν30) were mixed together. The torsion mode (through C1–N bond) of ν27 is only split to give positive Δω value of 6 cm^{-1} for group A. The in-phase motion (Raman active) of two torsions through C1–N bond in group A looks like a twist motion (consequently no dipole derivative) of methylene hydrogen atoms, and the out-of-phase motion (IR active) like a wagging motion (consequently small fluctuation of dipole) of those two. This difference induces the splitting of ν27 mode because the wagging is usually higher in frequency than the twisting motion.

Force constants of hydrogen bonding in local symmetry coordinate. The optimized structural parameters and calculated force constants in local symmetry coordinates of hydrogen bonding in DMF hexamer cluster using BP86 and B3LYP are shown in Table 4 along with crystal structural parameters available. Although the results of two methods are not much

different from another, the force constants calculated from BP86 functional are discussed as following because the calculated spectra using the functional BP86/6-31+G** fits well the experimental infrared and Raman spectra compared to results of B3LYP functional.

Stretching of hydrogen bonding: Force constants of slightly bent (~160 degree) and near (less 2.4 Å) H···O bonds (H18···O2 and O38···H10) which were drawn with dashed lines in Figure 1, came out to 0.081 and 0.1084 mdyn/Å. For further bent (~140 degree) and a little further apart (no less 2.5 Å) H···O bonds shown with dashed lines, O14···H55 and H43···O62, they were calculated to 0.055 and 0.0693 mdyn/Å. These values are about one fourth of strong hydrogen bonding chemical system. It is more than one half the stretching force constants 0.125 mdyn/Å of C=O···H–N in the polyglycine peptide system.[11] This outcome is quite similar to the result previously reported for DMF dimer system[8] where roughly one-half the strength of the C=O···H–N hydrogen bond was calculated. These values are quite comparable to 0.0582 mdyn/Å observed from a hydrogen-bonded dimer[29] formed between trimethylamine and acetylene, $(CH_3)_3N\cdots HC\equiv CH$, in gas phase by Fourier-transform microwave spectroscopy. The distance of the hydrogen bond is similar to 2.4 Å calculated in the hydrogen bonded system[30] of ammonia-acetylene dimer, $H_3N\cdots HC\equiv CH$.

In-plane bending of hydrogen bonding: Force constants of the in-plane bending of hydrogen bonding C13-H18···O2, which is quite crowd sterically than others, shows 0.5514 mdynÅ. However, other three bending motions give values in the range of ~0.3 mdynÅ. These are about one half of usual bending force constants observed in typical methyl group, but are quite large compared to 0.030 mdynÅ of C=O···H–N bending force constants[31] obtained from the calculation of crystalline antiparallel chain pleated sheet polyglycine I system. However, the bending force constants of weakly bound dimers in the gas phase[32] were obtained for a series of dimers, A···B (A: symmetric top, B: linear). For the dimer of $H_3N\cdots HCN$, it was calculated to $\sim 94 \times 10^{-21}$J from the gas phase nuclear quadrupole coupling constants. This corresponds to a value of ~0.094 mdynÅ. Because the hexamer structure has been connected each other through hydrogen bonding with next molecules in the cluster, these in-plane bending modes seem to be very rigid. Further, it has much heavier than small molecules. Recent study[33] of 15-base pair oligomer of single stranded nucleic acid fragments showed that the bending by 90º requires roughly 5 kcal mol^{-1} where the effective bending force constants of 0.02 ~ 0.06 kcal mol^{-1} $degree^{-2}$ was reported. This corresponds to roughly 0.46 ~ 1.4 mdynÅ which is yet very huge in fact.

Torsion of hydrogen bonding: Force constants of torsion modes of weakly bent hydrogen bonding came out about 0.09 mdynÅ, but of further bent hydrogen bonding to about 0.04 mdynÅ. These values are also several times larger than the usual torsion force constants adapted in the analysis of polyglycine I system. This is also mainly due to the rigidity in the hexamer cluster.

Conclusions

The equilibrium structure, the stabilization energies, and the vibrational properties were studied using a hexamer cluster of DMF molecules. Stabilization free energy for a hexamer formation was calculated to about –40 kJ/mol using B3LYP/ 6-31+G** and BP86/6-31+G** theory. This implies that DMF molecules in a condensed phase operate very strong intermolecular interactions. The interactions in bulk could be electrostatic, dipole-dipole or dispersive interaction. These nonbonding interactions are supposed to happen cooperatively through hydrogen atoms in bulk. This can be understood as weak or soft intermolecular hydrogen bonding, a type of C–H···O which can be regarded responsible partly for the hexamer cluster stabilization. Using the force constant matrix calculated for hexamer, vibrational analysis shows successful to explain the experimental Raman and infrared spectra of DMF liquid state. Noncoincidence in Raman and infrared frequencies of amide I band observed experimentally in the liquid state was interpreted in terms of intermolecular vibrational coupling of dipoles. This supports certain degree of ordering in the liquid state of DMF. The stretching and angle-bending force constants of intermolecular hydrogen bonds C–H···O were considerable to the extent that could not be neglected.

Acknowledgments. This work was supported by the research grant of the Chungbuk National University in 2007.

References

1. Borrmann, H.; Persson, I.; Sandström, M.; Stalhandske, C. M. V. *J. Chem. Soc., Perkin Trans.* **2000**, *2*, 393.
2. (a) Stalhandske, C. M. V.; Minkmm, J.; Sandström, M.; Papai, I.; Johansson, P. *Vib. Spectrosc.* **1997**, *14*, 207. (b) Durgaprasad, G.; Sathyanarayana, D. N.; Patel, C. C. *Bull. Chem. Soc. Jpn.* **1971**, *44*, 316.
3. Zhou, X.; Krauser, J. A.; Tate, D. R.; VanBuren, A. S.; Clark, J. A.; Moody, P. R.; Liu, R. *J. Phys. Chem.* **1996**, *100*, 16822.
4. (a) Radnai, T.; Itoh, S.; Othaki, H. *Bull. Chem. Soc. Jpn.* **1988**, *61*, 3845. (b) Othaki, H.; Itoh, S.; Rode, B. M. *Bull. Chem. Soc. Jpn.* **1986**, *59*, 271. (c) Othaki, H.; Itoh, S.; Yamaguchi, T.; Ishigro, S.; Rode, B. M. *Bull. Chem. Soc. Jpn.* **1983**, *56*, 3406.
5. Schultz, G.; Hargitti, I. *J. Phys. Chem.* **1993**, *97*, 4966.
6. Cordeiro, J. M. M. *Inter. J. Quan. Chem.* **1997**, *65*, 709.
7. Miyake, M.; Kaji, O.; Nakagawa, N.; Suzuki, T. *J. Chem. Soc., Faraday Trans. 2* **1985**, *81*, 277.
8. Vargas, R.; Garza, J.; Dixon, D. A.; Hay, B. P. *J. Am. Chem. Soc.* **2000**, *122*, 4750.
9. Kim, K. H.; Kim, Y. *Bull. Korean Chem. Soc.* **2007**, *28*, 2454.
10. Desiraju, G. R.; Steiner, T. *The Weak Hydrogen Bond in Structural Chemistry and Biology*; Oxford University Press: Oxford and New York, 1999.
11. Lee, S.-H.; Palmo, K.; Krimm S. *J. Comput. Chem.* **1999**, *20*, 1067.
12. Lee, C.; Park, S.-K.; Lee, Min, K.-C.; Kim, Y.; Lee, N.-S. *Bull. Korean Chem. Soc.* **2008**, *29*, 1951.
13. Giorgini, M. G.; Musso, M.; Asenbaum, A.; Döge, G. *Mol. Phys.* **2000**, *98*, 783.
14. (a) Kirillov, S. A. *J. Mol. Liq.* **2004**, *110*, 95. (b) Giorgini, M. G. *Pure Appl. Chem.* **2004**, *76*, 157.
15. (a) Musso, M.; Giorgini, M. G.; Torii, H.; Dorka, R.; Schiel, D.; Asenbaum, A.; Keutel, Z.; Oehme, K.-L. *J. Mol. Liq.* **2006**, *125*, 115. (b) Torii, H.; Musso, M.; Giorgini, M. G. *J. Phys. Chem. A* **2005**, *109*, 7797.
16. Torii, H. *J. Phys. Chem. B* **2007**, *111*, 5434.
17. (a) Torii, H. *J. Phys. Chem. A* **1999**, *103*, 2843. (b) Musso, M.; Torii, H.; Ottaviani, P.; Asenbaum, A.; Giorgini, M. G. *J. Phys. Chem. A* **2002**, *106*, 10152.

18. (a) Torii, H. *J. Phys. Chem. A* **2006**, *110*, 4822. (b) Torii, H. *Chem. Phys. Lett.* **2005**, *414*, 417.
19. Dub, P. A.; Filippov, O. A.; Belkova, N. V.; Rodriguez-Zubiri, M.; Poli, R. *J. Phys. Chem. A* **2009**, *113*, 6348.
20. Myshakina, N. S.; Asher, S. A. *J. Phys. Chem. B* **2007**, *111*, 4271.
21. Meic, Z.; Baranovic, G.; Smrecki, V.; Novak, P.; Keresztury, G.; Holly, H. *J. Mol. Str.* **1997**, *408/409*, 399.
22. Michalska, D.; Bienko, D. C.; Czarnik-Matusewicz, B.; Wierzejewska, M.; Sandorfy, C.; Zeegers-Huyskens, Th. *J. Phys. Chem. B* **2007**, *111*, 12228.
23. Jabłonski, M. *J. Mol. Struct. (Theochem)* **2007**, *820*, 118.
24. Katsumoto, Y.; Komatsu, H.; Ohno, K. *J. Am. Chem. Soc.* **2006**, *128*, 9278.
25. Xu, Z.; Li, H.; Wang, C.; Wu, T.; Han, S. *Chem. Phys. Lett.* **2004**, *394*, 405.
26. Biliskov, N.; Baranovic, G. *J. Mol. Liq.* **2009**, *144*, 155.
27. Xu, Z.; Li, H.; Wang, C.; Pan, H.; Han, S. *J. Chem. Phys.* **2006**, *124*, 244502.
28. Lei, Y.; Li, H.; Pan, H.; Han, S. *J. Phys. Chem. A* **2003**, *107*, 1574.
29. Legon, A. C.; Rego, C. A. *J. Mol. Struct.* **1988**, 189, 137.
30. Hartmann, M.; Radom, L. *J. Phys. Chem. A* **2000**, *104*, 968.
31. Moore, W. H.; Krimm, S. *Proc. Nat. Acad. Sci. USA* **1975**, *72*, 4933.
32. (a) Legon, A. C.; Lister, D. G. *J. Mol. Struct.* **1996**, *382*, 63. (b) Legon, A. C.; Cope, P.; Millen, D. J. *J. Chem. Soc., Perkin Trans.* **1986**, *82*, 1189.
33. Curuksu, J.; Zacharias, M.; Lavery, R.; Zakrzewska, K. *Nucleic Acids Res*. **2009**, *37*, 3766.